Materials Advances

ROYAL SOCIETY OF CHEMISTRY

PAPER

View Article Online
View Journal | View Issue

Cite this: *Mater. Adv.*, 2021, 2, 4333

Malleable and recyclable imide–imine hybrid thermosets: influence of imide structure on material property†

Xiran Shen,[a] Yunlong Ma,[a] Shichang Luo,[a] Rao Tao,[a] Dan An,[a] Xinlei Wei,[a] Yinghua Jin,[b] Li Qiu*[a] and Wei Zhang*[b]

Received 6th April 2021,
Accepted 23rd May 2021

DOI: 10.1039/d1ma00311a

rsc.li/materials-advances

Although thermosetting polyimides have been widely used in many fields, it is still a challenging task to realize their repairability, reprocessibility, and recyclability, which are highly desirable in mitigating the cost and environmental concern. In this work, a series of malleable imide–imine hybrid thermosets were prepared through imine condensation of amino-terminated imide macromonomers with a dialdehyde and triamine crosslinker. Such novel hybrid materials exhibit rehealability and recyclability enabled by the dynamic imine bonds, while retaining the excellent mechanical and thermal properties of polyimide. Success here not only expands the library of building blocks for preparation of repairable and recyclable polyimides targeting different applications, but also opens new possibilities for reprocessing thermosetting polymers and developing high-performance dynamic covalent hybrid polymeric materials.

Introduction

A hybrid material consisting of two or more constituents blended on the molecular level usually shows characteristics in between those of the original constituents,[1] allowing "performance integration" in a single material.[2–4] With the need and advent of various smart/multifunctional materials, efficient and feasible hybridization strategies have attracted increasing attention.[5,6] Particularly, hybridization of classic thermosetting polymers (*i.e.*, highly cross-linked covalent network polymers) by incorporating dynamic covalent bonds represents a rapidly emerging and practical chemical approach, which can lead to the formation of a novel class of polymers referred to as "covalent adaptable networks" (CANs). Consisting of dynamic covalent crosslinks, CANs combine excellent mechanical properties of thermosets with reprocessability, rehealability, and recyclability of thermoplastics.[7–9] Since the first example of a Diels–Alder reaction based CAN was reported in 2002,[10] various reversible reactions such as transesterification,[11–13] olefin metathesis,[14–16] disulfide chemistry,[17–19] boronic acid chemistry[20–22] and Schiff base reaction[23,24] have been employed for the CAN preparation. Among them, polyimines (PIs) prepared *via* Schiff base reactions are of particular interest due to readily available starting materials, straightforward synthesis, and excellent rehealability, reprocessability, and recyclability.[24–28] Commercially available thermosetting polyimides (PIms) are a class of widely used polymers, which contain cyclic imide moieties in their backbones.[29] Their rigid backbones give them excellent mechanical properties, dielectric properties, and resistance to radiation and high temperature, thus leading to a broad range of applications in liquid crystal,[30] separation film,[31] flexible printed circuit,[32] battery,[33] organic light-emitting diode,[34] optical fiber,[35] and other fields. However, at present, PIms are mainly produced as thermosetting materials. Therefore, any damages or structural defects cannot be repaired, and it is also challenging to reprocess and recycle these thermosets, which strongly impede their sustainable development. To overcome these challenges, hybridization of PIms by incorporating dynamic covalent bonds into the polymer backbone represents a promising solution.

Previously, as a proof-of-concept study, we demonstrated the excellent mechanical properties, rehealability and recyclability of an imide–imine hybrid polymer, which proved the feasibility of the hybridization strategy.[36] The strategy introduces dynamic imine bonds into the PIm backbone to realize the hybridization of PI and PIm at the molecular level. Consequently, the resulting organic hybrid materials exhibit the advantages of both PI (reprocessability, self-healing, and recycling properties) and PIm (excellent mechanical and thermal properties). However, the scope of such bottom-up hybridizing approach and the structure–property relationship of this novel class of hybrid malleable thermosets are still not clear, thus lacking practical guidelines for rational structural design. Given the easy

[a] *Yunnan Key Laboratory for Micro/Nano Materials & Technology, National Center for International Research on Photoelectric and Energy Materials, School of Materials and Energy, Yunnan University, Kunming 650091, P. R. China. E-mail: qiuli@ynu.edu.cn*

[b] *Department of Chemistry, University of Colorado, Boulder, Colorado 80309, USA. E-mail: wei.zhang@colorado.edu*

† Electronic supplementary information (ESI) available: Synthesis details, spectroscopic and mechanical characterization, *etc*. See DOI: 10.1039/d1ma00311a

accessibility of the imides and imines, such hybridization strategy could pave a way toward malleable PIm thermosets with a wide range of mechanical and thermal properties. We herein report a systematic study on the scope of this hybridization strategy to demonstrate its general applicability and the tunability of mechanical and thermal properties of the novel imine–imide hybrid thermosets.

Results and discussion

The poly(imide–imine) (PIm–PI) hybrid materials were prepared as thin films instead of powder samples to facilitate the subsequent sample characterization. Three dianhydrides including 4,4′-(hexafluoroisopropylidene)diphthalic anhydride (6FDA), 4,4′-oxydiphthalic anhydride (ODPA), and 3,3′,4,4′-benzophenone tetracarboxylic dianhydride (BTDA), and two diamines (2,6-diaminotoluene (DAT)), 2,5-dimethyl-1,4-phenylenediamine (DPD) were selected as the building blocks to synthesize the amine-terminated imide monomers (FDA-DAT, ODPA-DAT, BTDA-DAT, FDA-DPD, ODPA-DPD, BTDA-DPD, details shown in the ESI†). The imide-based diamine monomers were then subjected to imine condensation with other aldehyde and amine monomers to form the PIm–PI films (Hy-FDA-DAT, Hy-ODPA-DAT, Hy-BTDA-DAT, Hy-FDA-DPD, Hy-ODPA-DPD, Hy-BTDA-DPD, Scheme 1). The hybrid polymers were obtained as yellow films through solvent annealing method under gradient heating (Details shown in the ESI†). The resulting polymer films were further heat-pressed (65 °C for 1–2 h and 75 °C for 1–2 h) under nominal contact pressure until the sample mass stayed constant. Six bright yellow thin films were finally obtained. Both FT-IR (Fig. S3, ESI†) and solid-state ^{13}C NMR spectroscopy (Fig. S4, ESI†) analysis support the anticipated chemical structures of the six hybrid poly(imide–imine)s. The disappearance of the stretching vibration peak of the aldehyde groups and the appearance of the imine bond stretching band confirm the efficient polymerization process. Both the band at 1375 cm^{-1} due to C–N–C stretching vibration, and the ones at ∼1718 cm^{-1} and 1782 cm^{-1} originated from the imide carbonyl groups confirm the formation of five-membered imide rings,[36] while the band at ∼1640 cm^{-1} due to –C═N– stretching mode indicates the successful formation of imine linkages. In addition, for all the six PIm–PIs, there is no peak at ∼1700 cm^{-1} corresponding to the aldehyde functional groups. The solid state ^{13}C NMR characterization also shows no or feeble signal at 190 ppm corresponding to the aldehyde groups, further indicating the high conversion of the aldehyde monomers. All the films showed a uniform thickness as measured (randomly choosing 5–10 sites in the film) with a thickness gauge, which demonstrates the procedure we employed for the film preparation could provide good quality films for mechanical measurement. The characterization of the surface morphology of the films with atomic force microscopy (AFM) revealed excellent surface smoothness (Fig. S5, ESI†). Furthermore, the surface morphologies were independent of the imide substrates, which could thus rule out the effect of morphology on the material performance difference.

With a series of hybrid materials in hand, we next tested and compared the mechanical properties of the as-obtained PIm–PIs films. All the tensile tests were performed at a tensile speed of 2 mm min^{-1} and each test was repeated at least 3 times with different samples (Fig. 1). Table 1 shows the performance of the six hybrid films with different imide fragments. To make a fair comparison, the molar ratio of imide to imine moiety was fixed to 1 : 4, and the degree of crosslinking was set to 50% (ESI†). All hybrid films exhibit good thermal properties with glass transition temperature (T_g) higher than 130 °C and thermal decomposition temperature higher than ∼200 °C. Furthermore, all the polymers showed high tensile strength (58–79 MPa) and tensile modulus (1.79–2.49 GPa), which are comparable to many existing polyimides (tensile strength 70–100 MPa, tensile modulus 1.5–3.0 GPa)[29] but superior to many polyimines.[25,26,37–40] These results indicate that the hybridization by integrating the imine bond into the polyimide backbone does not adversely lead to reduction in mechanical properties of polyimides. Furthermore, the tensile strength and moduli of all the PIm–PIs are 50–100% higher in comparison with those of the polyimine with the same crosslinking density of 50% (PI, 37 MPa and 1.22 GPa, respectively, Table 1), indicating the rigid imide structure could significantly improve the mechanical properties. By comparing the following three pairs of samples: Hy-FDA-DAT *vs.* Hy-FDA-DPD; Hy-ODPA-DAT *vs.* Hy-ODPA-DPD; Hy-BTDA-DAT *vs.* Hy-BTDA-DPD, we found when the selected dianhydride building blocks are the same, the hybrids prepared with the linear paraphenylenediamine (DPD) are mechanically stronger than those prepared with *meta*-substituted phenylene diamine (DAT). This is likely due to (1) the additional methyl substituent in DPD hinders chain motion, thus providing a more rigid structure;[41] (2) *para*-substituted diamine

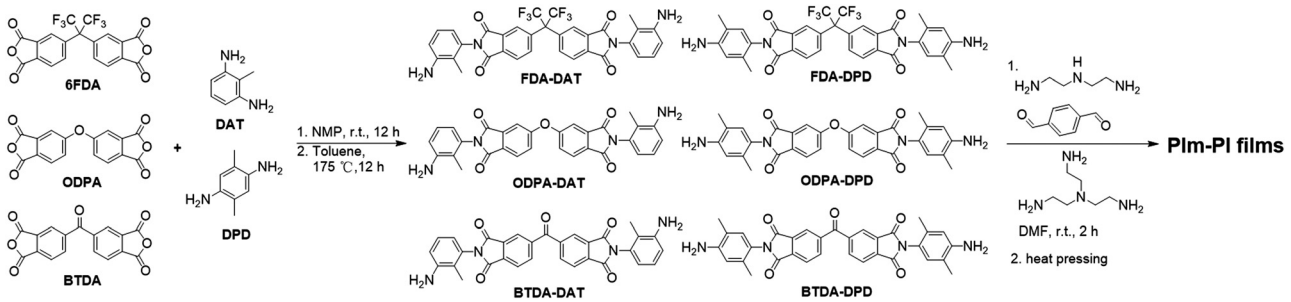

Scheme 1 Synthesis of six amino-terminated imide monomers and corresponding PIm–PI films.

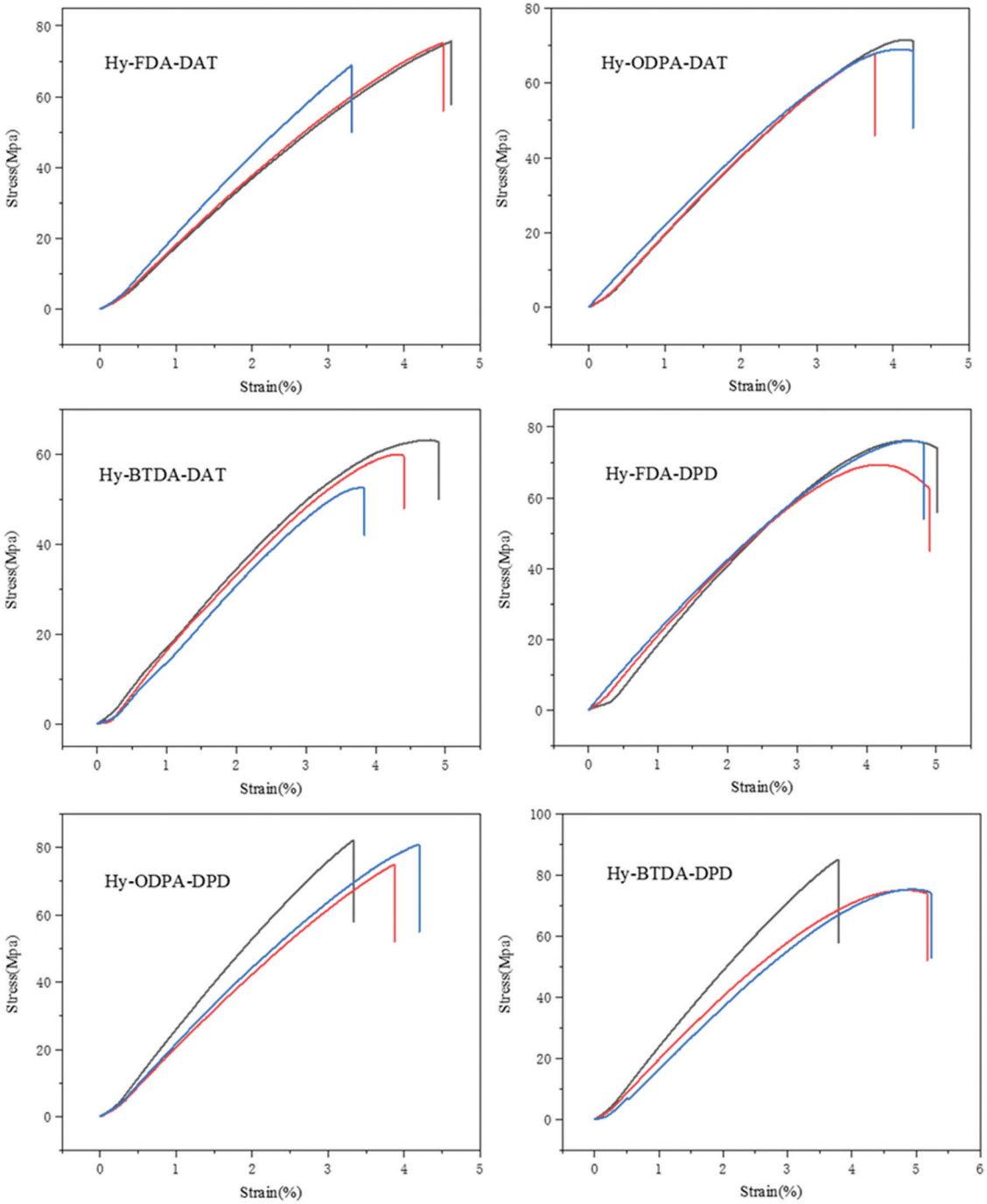

Fig. 1 Tensile stress–strain curves of the as-synthesized hybrid films. Three different samples were tested for each material.

DPD gives higher chain linearity than *meta*-substituted diamine DAT, which could facilitate the π–π interactions between the molecular chains.[42] The rigidity of the dianhydride monomers follows the order of BTDA > 6FDA > ODPA.[41,43] The least rigid ODPA moieties have a slightly positive effect on the mechanical properties when compared to FDA and BTDA. Besides the mechanical properties, the thermal properties of the imide–imine hybrid polymers were also assessed through DMA and TGA characterizations (Fig. S7, S8 and Table S1, ESI†), and the relevant parameters are summarized in Table 1. The T_g of all the samples is in the range of 137–161 °C. Again, the polymers composed of linear paraphenylenediamine DPD have higher T_g than their analogues consisting of metaphenylenediamine DAT: Hy-FDA-DAT < Hy-FDA-DPD; Hy-ODPA-DAT < Hy-ODPA-DPD; Hy-BTDA-DAT ≈ Hy-BTDA-DPD. This is again likely due to higher chain rigidity and linearity provided by DPD compared to DAT, basically agreeing with the general knowledge that more rigid and linear polymer chain usually leads to a higher T_g of the material.[41,43] The T_g of these hybrid PIm–PIs with rigid imide moieties is around two-fold higher than that of the polyimine (PI, 75 °C).

Table 1 The mechanical and thermal properties of six hybrid films

Polymer	Tensile strength[a] (MPa)	Tensile modulus[a] (GPa)	Elongation at break[a] (%)	T_g (°C)	T_d @5 wt% weight loss (°C)
Hy-FDA-DAT	73.19 ± 3.10	2.11 ± 0.17	4.15 ± 0.59	144	208
Hy-ODPA-DAT	69.37 ± 1.64	2.16 ± 0.04	4.10 ± 0.24	137	200
Hy-BTDA-DAT	58.51 ± 4.51	1.79 ± 0.09	4.38 ± 0.44	155	203
Hy-FDA-DPD	73.85 ± 3.20	2.23 ± 0.08	4.92 ± 0.08	161	210
Hy-ODPA-DPD	79.22 ± 3.15	2.49 ± 0.23	3.80 ± 0.36	142	196
Hy-BTDA-DPD	78.45 ± 4.55	2.23 ± 0.33	4.73 ± 0.67	156	206
PI	36.85 ± 0.27	1.22 ± 0.07	4.34 ± 0.32	75	187

[a] Tensile measurement was carried out on 3 spindle film strips (width: 3.23 mm, thickness: 0.22–0.3 mm, length: 20–26 mm of the middle rectangular part) with a crosshead speed of 2 mm min^{-1}.

Generally, traditional thermosetting polymers are insoluble and infusible upon crosslinking and curing, and thus cannot be reshaped. By contrast, crosslinked CANs can be reshaped and repaired through bond exchange reactions, which significantly broadens the application potential of thermoset polymers and benefits their sustainable development.[12,44,45] The previous reports demonstrated that the dual action of heating and pressure can effectively accelerate the imine exchange reaction in polyimines, thus enabling their reprocessibility and repairability.[24,28,46] The repairability and recyclability of PIm–PIs were thus explored. Following a similar procedure for polyimines reported by our team,[28,47] a piece of PIm–PI was cut into two pieces, which were then put together in contact with a crack width of ~400 μm. To the contact area was added a drop (~25 μL) of diethylenetriamine (DETA) solution in acetonitrile/DMF (v/v = 1:1, 10 mg mL^{-1}). The sample was then heat-pressed using a temperature program (50 °C, 60 °C, 80 °C, 2 hours for each temperature) to completely heal the cut. As shown in Fig. 2, the sample was fractured at a different position rather than where the original cut was healed, indicating the good healing efficiency. The mechanical properties of the repaired films are shown in Fig. 3a. The repair efficiencies of all the samples are in the range of 94–106% based on tensile moduli, demonstrating the superior rehealability of the PIm–PI hybrid polymers enabled by the dynamic imine bonds. The recovery of the tensile strength and elongation at break were in the range of 74–96% and 66–103%, respectively (Table S2, ESI†).

So far, we have shown that such hybridization strategy can effectively retain the mechanical properties and thermal stability of PIm while bringing in the repairability of PI. In order to demonstrate the general recyclability of PIm–PI hybrid materials through transimination-triggered depolymerization process, all the six samples were studied following the procedure shown below: PIm–PI was soaked in the DMF solution containing DETA and tris(2-aminoethyl)amine (TREN), which was then heated at 55 °C for 2 h. All the six PIm–PI samples were gradually dissolved to eventually form a completely homogeneous and clear solution. The full recyclability of Hy-ODPA-DAT and Hy-BTDA-DAT were exemplified. Fresh TPA and ODPA-DAT (or BTDA-DAT) monomers were added to the clear depolymerized solution of Hy-ODPA-DAT (or Hy-BTDA-DAT), which was then poured into a flat glass dish after thoroughly mixing. The first-generation film was obtained following the procedure described in the previous work.[36] Hy-ODPA-DAT and Hy-BTDA-DAT were recycled two more times to give the second and third-generation recycled Hy-ODPA-DAT and Hy-BTDA-DAT. As shown in Fig. 3b (for Hy-ODPA-DAT) and Fig. S13 (ESI†) (for Hy-BTDA-DAT), no obvious loss but slight improvement in mechanical property (based on tensile modulus) was observed for the recycled samples. Therefore, the results verify the degradability and recyclability of the PIm–PI hybrid polymers.

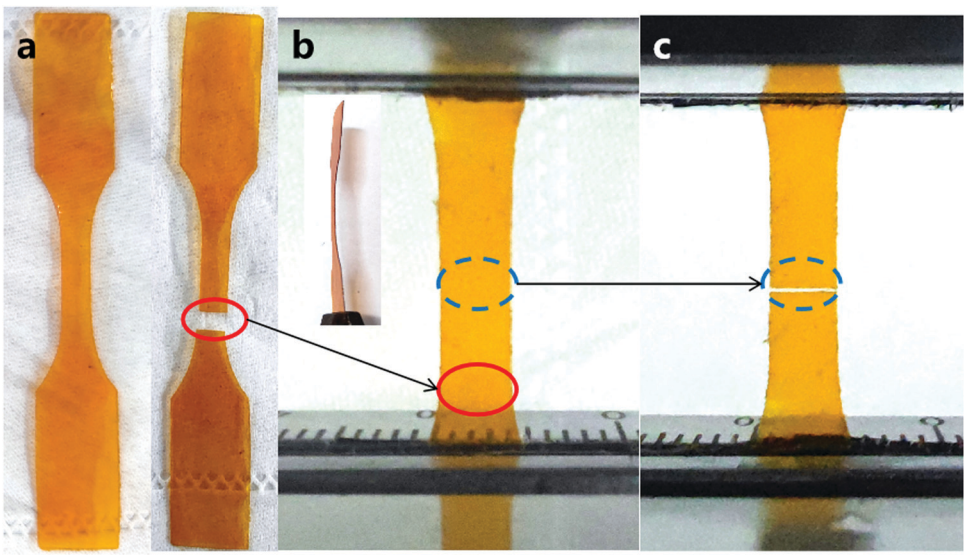

Fig. 2 The optical images of the PIm–PI (Hy-ODPA-DAT) film before ((a) left: as-synthesized, right: cut piece) and after heat-pressing (b), and after the second tensile testing (c). The rehealed positions are indicated by the red circles, and the dashed blue circles indicate the new fractured locations.

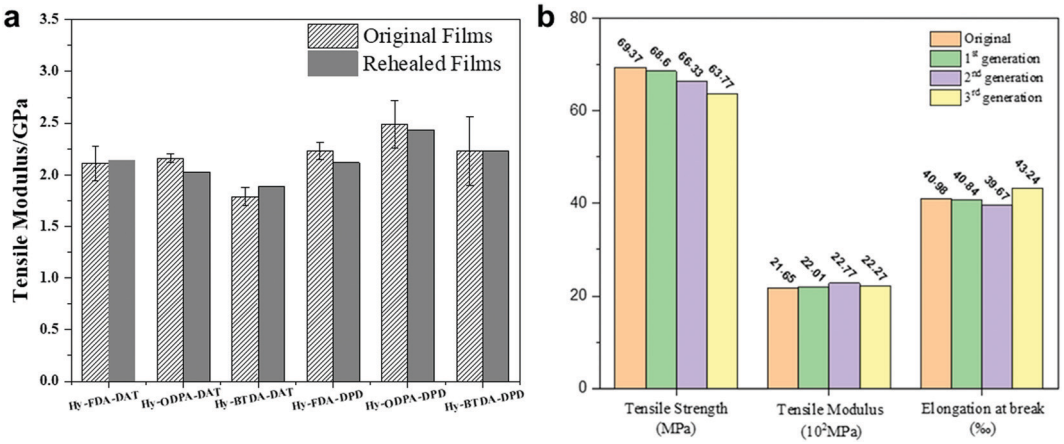

Fig. 3 (a) Tensile moduli of six hybrid films before and after repairing; (b) mechanical properties of Hy-ODPA-DAT after three generation recycling.

Conclusions

In summary, by integrating dynamic imine bonds with imide building blocks, a series of PIm–PI hybrid materials have been prepared. Thanks to the dynamic nature of the imine bond, the resulting PIm–PIs are malleable, rehealable and recyclable. The mechanical and thermal properties can be fine-tuned by varying the monomer structures. The study showed that the more rigid monomer precursor (mainly decided by the amine moiety in the imide) led to better mechanical performance and higher T_g. The molecular-level hybridization strategy reported herein will open new possibilities for reprocessing of thermosetting polymers and development of novel CANs.

Experimental section

Synthesis of Ims

At room temperature, the diamine (13.5 mmol) and dianhydride (4.5 mmol) were mixed in *N*-methylpyrrolidone (NMP, 50 mL) under nitrogen atmosphere. After stirring for 12 h at room temperature, toluene (16 mL) was added. The solution was heated at 175 °C for 10 h, during which time water was removed with the use of a Dean–Stark trap. After cooling to room temperature, the mixed solution was added dropwise to water and methanol (500 mL, v/v = 1 : 1) with vigorous stirring. The mixture was allowed to stand for 1 h until the solid completely precipitated out. The precipitates were collected by centrifugation and suction filtration. The collected dark brown solid was dried under vacuum at 65 °C, and finally separated and purified by column chromatography (eluent: CH_2Cl_2/CH_3OH = 180 : 1) to obtain the pure product.

Preparation of PIm–PIs films

The molar ratio of imide : imine groups was fixed to 1 : 4 in all the polymers. The molar percentage of the crosslinking amine moieties in the total primary amines in the resulting polymer network (denoted as crosslinking density) was fixed to 50%. Imide monomers Im, tris(2-aminoethyl)amine (TREN) and diethylenetriamine (DETA) were uniformly dispersed in DMF in 3 : 3 : 4 equivalents. A solution of TPA in DMF was added into the above solution. The solution was poured into a dust-free glass dish. After two hours, the solution turned into a completely opaque gel state. The gel was kept at room temperature for 2 h, and the resulting film was then heated on a flat heating device at 50 °C for 12 h, and kept at 60 °C, 80 °C, 100 °C and 120 °C for 2 h at each temperature. After soaking in deionized water at room temperature to demold, the film was transferred to a vacuum oven and kept at 65 °C overnight. The obtained films were finally heat-pressed at 65 °C for 2 h and 75 °C for 2 h to give a smooth and transparent organic hybrid film.

Recycling of hybrid films

The recycling procedure reported previously was followed.[24,36]

Conflicts of interest

The authors declare no conflicts of interest.

Acknowledgements

This work was financially supported by University of Colorado Boulder, National Science Foundation of China (21875208), and Yunnan University (WX160117, C176220100005).

Notes and references

1 G. Kickelbick, *Hybrid materials: synthesis, characterization, and applications*, John Wiley & Sons, 2007.
2 G. Chang, L. Yang, J. Yang, M. P. Stoykovich, X. Deng, J. Cui and D. Wang, *Adv. Mater.*, 2018, **30**, 1704234.
3 C. Bao, Z. Guo, H. Sun and J. Sun, *ACS Appl. Mater. Interfaces*, 2019, **11**, 9478–9486.
4 X. Lu, Y. Luo, Y. Li, C. Bao, X. Wang, N. An, G. Wang and J. Sun, *CCS Chem.*, 2020, **2**, 524–532.
5 I. Cobo, M. Li, B. S. Sumerlin and S. Perrier, *Nat. Mater.*, 2015, **14**, 143–159.

6 H. Zhang, Y. Liu, D. Yao and B. Yang, *Chem. Soc. Rev.*, 2012, **41**, 6066–6088.
7 M. Guerre, C. Taplan, J. M. Winne and F. E. Du Prez, *Chem. Sci.*, 2020, **11**, 4855–4870.
8 Y. Jin, Z. Lei, P. Taynton, S. Huang and W. Zhang, *Matter*, 2019, **1**, 1456–1493.
9 C. J. Kloxin and C. N. Bowman, *Chem. Soc. Rev.*, 2013, **42**, 7161–7173.
10 X. Chen, M. A. Dam, K. Ono, A. Mal, H. Shen, S. R. Nutt, K. Sheran and F. Wudl, *Science*, 2002, **295**, 1698.
11 J. P. Brutman, P. A. Delgado and M. A. Hillmyer, *ACS Macro Lett.*, 2014, **3**, 607–610.
12 M. Capelot, D. Montarnal, F. Tournilhac and L. Leibler, *J. Am. Chem. Soc.*, 2012, **134**, 7664–7667.
13 D. Montarnal, M. Capelot, F. Tournilhac and L. Leibler, *Science*, 2011, **334**, 965–968.
14 Y.-X. Lu and Z. Guan, *J. Am. Chem. Soc.*, 2012, **134**, 14226–14231.
15 Y.-X. Lu, F. Tournilhac, L. Leibler and Z. Guan, *J. Am. Chem. Soc.*, 2012, **134**, 8424–8427.
16 J. A. Neal, D. Mozhdehi and Z. Guan, *J. Am. Chem. Soc.*, 2015, **137**, 4846–4850.
17 L. Imbernon, E. K. Oikonomou, S. Norvez and L. Leibler, *Polym. Chem.*, 2015, **6**, 4271–4278.
18 A. Ruiz de Luzuriaga, R. Martin, N. Markaide, A. Rekondo, G. Cabañero, J. Rodríguez and I. Odriozola, *Mater. Horiz.*, 2016, **3**, 241–247.
19 A. Takahashi, T. Ohishi, R. Goseki and H. Otsuka, *Polymer*, 2016, **82**, 319–326.
20 A. P. Bapat, D. Roy, J. G. Ray, D. A. Savin and B. S. Sumerlin, *J. Am. Chem. Soc.*, 2011, **133**, 19832–19838.
21 W. L. A. Brooks and B. S. Sumerlin, *Chem. Rev.*, 2016, **116**, 1375–1397.
22 O. R. Cromwell, J. Chung and Z. Guan, *J. Am. Chem. Soc.*, 2015, **137**, 6492–6495.
23 M. E. Belowich and J. F. Stoddart, *Chem. Soc. Rev.*, 2012, **41**, 2003–2024.
24 P. Taynton, H. Ni, C. Zhu, K. Yu, S. Loob, Y. Jin, H. J. Qi and W. Zhang, *Adv. Mater.*, 2016, **28**, 2904–2909.
25 P. Taynton, K. Yu, R. K. Shoemaker, Y. Jin, H. J. Qi and W. Zhang, *Adv. Mater.*, 2014, **26**, 3938–3942.
26 C. Zhu, C. Xi, W. Doro, T. Wang, X. Zhang, Y. Jin and W. Zhang, *RSC Adv.*, 2017, **7**, 48303–48307.
27 R. Mo, J. Hu, H. Huang, X. Sheng and X. Zhang, *J. Mater. Chem. A*, 2019, **7**, 3031–3038.
28 P. Taynton, C. Zhu, S. Loob, R. Shoemaker, J. Pritchard, Y. Jin and W. Zhang, *Polym. Chem.*, 2016, **7**, 7052–7056.
29 D.-J. Liawa, K.-L. Wangb, Y.-C. Huanga, K.-R. Leec, J.-Y. Laic and C.-S. Had, *Prog. Polym. Sci.*, 2012, 907–974.
30 B. Chae, S. B. Kim, S. W. Lee, S. I. K. W. Choi, B. Lee, M. Ree, K. H. Lee and J. C. Jung, *Macromolecules*, 2002, 10119–10130.
31 H. Sanaeepur, A. Ebadi Amooghin, S. Bandehali, A. Moghadassi, T. Matsuura and B. Van der Bruggen, *Prog. Polym. Sci.*, 2019, **91**, 80–125.
32 H. Yousef, K. Hjort and M. Lindeberg, *J. Microelectromech. Syst.*, 2007, **16**, 1341–1348.
33 Z. Song, H. Zhan and Y. Zhou, *Angew. Chem., Int. Ed.*, 2010, **49**, 8444–8448.
34 J. Shen, F. Li, Z. Cao, D. Barat and G. Tu, *ACS Appl. Mater. Interfaces*, 2017, **9**, 14990–14997.
35 P. J. Thomas and J. O. Hellevang, *Sens. Actuators, B*, 2018, **270**, 417–423.
36 X. Lei, Y. Jin, H. Sun and W. Zhang, *J. Mater. Chem. A*, 2017, **5**, 21140–21145.
37 R. Hajj, A. Duval, S. Dhers and L. Avérous, *Macromolecules*, 2020, **53**, 3796–3805.
38 Z. Zhou, X. Su, J. Liu and R. Liu, *ACS Appl. Polym. Mater.*, 2020, **2**, 5716–5725.
39 S. Luo, Y. Ma, X. Wei, Y. Jin, L. Qiu and W. Zhang, *ACS Appl. Electron. Mater.*, 2021, **3**, 1178–1183.
40 P. Taynton, C. Zhu, S. Loob, R. Shoemaker, J. Pritchard, Y. Jin and W. Zhang, *Polym. Chem.*, 2016, **7**, 7052–7056.
41 Y. Zhuang, J. G. Seong, Y. S. Do, W. H. Lee, M. J. Lee, M. D. Guiver and Y. M. Lee, *J. Membr. Sci.*, 2016, **504**, 55–65.
42 Q. Wang, Y. Bai, Y. Chen, J. Ju, F. Zheng and T. Wang, *J. Mater. Chem. A*, 2015, **3**, 352–359.
43 D. H. Wang, J. J. Wie, K. M. Lee, T. J. White and L.-S. Tan, *Macromolecules*, 2014, **47**, 659–667.
44 C. J. Kloxin, T. F. Scott, B. J. Adzima and C. N. Bowman, *Macromolecules*, 2010, **43**, 2643–2653.
45 M. Podgorski, B. D. Fairbanks, B. E. Kirkpatrick, M. McBride, A. Martinez, A. Dobson, N. J. Bongiardina and C. N. Bowman, *Adv. Mater.*, 2020, **32**, e1906876.
46 P. Taynton, K. Yu, R. K. Shoemaker, Y. Jin, H. J. Qi and W. Zhang, *Adv. Mater.*, 2014, **26**, 3938–3942.
47 J. Zhang, Z. Lei, S. Luo, Y. Jin, L. Qiu and W. Zhang, *ACS Appl. Nano Mater.*, 2020, **3**, 4845–4850.